

Highly sensitive and stable nanocage TiN SERS substrate synthesized via a facile hydrothermal method

YUN ZHOU^{1,2,*}, JIAN CHAI¹, XINQIAO TENG²

¹*Department of Public Basic Education, Zhejiang Polytechnic University of Mechanical and Electrical Engineering, Hangzhou 310053, China*

²*College of Science, China Jiliang University, Hangzhou 310018, China*

Titanium nitride (TiN) is a promising candidate for surface-enhanced Raman scattering substrates due to its highly metallic behavior, strong surface plasmon resonance, and good chemical stability. In this research, we developed a novel nanocage-structured TiN through a two-step synthesis protocol involving hydrothermal growth of titanium precursors followed by controlled ammonia nitridation. Comprehensive material characterization using SEM, XRD, and XPS revealed well-defined nanocage morphology with face-centered cubic crystalline structure and stoichiometric Ti/N ratio. Remarkably, the nanocage architecture TiN demonstrated intensified localized surface plasmon resonance (LSPR) effects across visible to near-infrared spectra, translating to superior SERS performance with detection sensitivity reaching 10^{-11} M for bisphenol A. Furthermore, nanocage TiN exhibits excellent resistance to acid–base corrosion, thus rendering it suitable for use as substrates in acid–base environments.

(Received August 26, 2025; accepted December 2, 2025)

Keywords: Nanocage structure, Hydrothermal method, Surface-enhanced Raman scattering, Raman detection

1. Introduction

Surface-enhanced Raman scattering (SERS) can greatly enhance the weak Raman signal of molecules, which makes it a very sensitive non-destructive analysis technique at trace level [1]. SERS can detect Raman signals from low-concentration materials and has been used as a powerful ultrasensitive optical detection method. Excellent SERS substrates should have the advantages of low cost, high chemical stability, good biocompatibility, and more importantly, strong resonance with the analyte [2]. Traditional noble metal SERS materials based on nanostructures with strong surface plasmon resonance (SPR), and electromagnetic mechanism (EM) are considered to be the main contribution to Raman enhancement [3]. In recent years, transition metal nitrides have attracted growing research interest due to their excellent surface catalytic activity, thermal stability and chemical stability. Among them, transition metals such as VN [4], WN [5] and MoN [6] exhibit excellent SERS performance. For example, Guan et al. reported that ultrathin δ-MoN nanosheets were synthesized by solution route at 270°C and 12 atm, and their Raman enhancement factor (EF) was determined to be 8.16×10^6 [7]. George et al. found that a few layered Ti₂N-MXenes exhibited ultrasensitive detection of certain explosives at the micromolar level [8]. Xi et al. developed a molten salt method to prepare plasma vanadium nitride porous materials, which can be used as sensitive and stable SERS substrates [4]. At present, the research on SERS substrates

mainly focuses on molybdenum nitride, vanadium nitride and tungsten nitride. However, there are few studies on TiN Raman enhancement. The previous research results show that porous TiN nanosheet-based substrate exhibited excellent enhancement effects for a minimum detectable concentration of 10^{-12} M [9]. TiN is an important functional material due to its strong surface plasmon resonance, high conductivity, excellent thermal stability and chemical stability [9]. However, due to its harsh reaction conditions, the synthesis of large-scale morphology-controllable transition metal TiN is still challenging. Therefore, research on TiN materials with other structures as SERS substrates has significant application value, offering a new type material for improving SERS technology. In this research, we propose a targeted etching preparation method to synthesize nanocage TiN hollow spheres with adjustable particle size. Nanocage TiN was obtained by nitriding TiO₂ hollow spheres in a nitrogen atmosphere. The reported TiN in this paper shows a strong localized surface plasmon resonance (SPR) effect in the visible light region. Additionally, the substrate exhibited excellent sensitivity, chemical stability and reproducibility, with a detection limit of 10^{-11} M.

2. Experimental details

A schematic diagram of nanocage TiN nanospheres synthesis method is shown in Fig. 1. After the synthesis of amorphous TiO₂ nanospheres TiO₂ by hydrothermal

method, in order to obtain nanocage TiN, the following two steps were required: etching and subsequent nitridation of amorphous hydrated TiO_2 sphere arrays.

Amorphous TiO_2 nanospheres were prepared as follows: At room temperature, 0.38 g of 28% $\text{NH}_3 \cdot \text{H}_2\text{O}$ solution and 0.91 g of H_2O were added to a mixed solution containing 300 mL ethanol ($\text{C}_2\text{H}_6\text{O}$) and acetonitrile ($\text{C}_2\text{H}_3\text{N}$) (volume ratio of 7:3), and the PH value was 5.

Under continuous stirring, 5 mL tetrabutyl titanate was immediately added to the above solution, thereby forming a milky white suspension within 2 s. After the suspension was continuously stirred for 24 h, the product formed by centrifugation was washed twice with ethanol to remove the unreacted precursor, and finally the sample was rinsed twice with water.

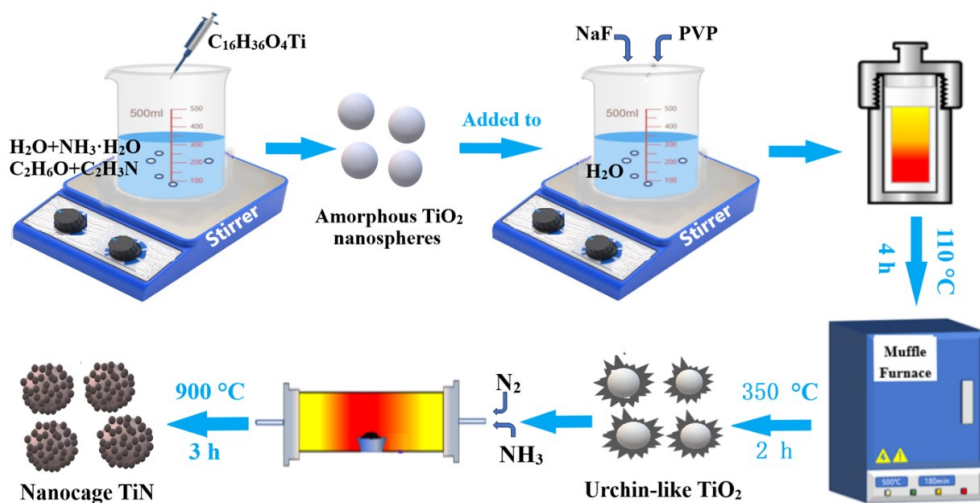


Fig. 1. Schematic diagram of TiN synthesis method (colour online)

The synthesis of hollow urchin-like TiO_2 was as follows: 1.5 g of amorphous TiO_2 nanospheres were redispersed in 30 mL water. Subsequently, 0.13 g of NaF was added as an etchant. After stirring for 1 h, 0.15 g of polyvinylpyrrolidone (PVP) with an average molecular weight (AMW) of 10 K was added. The suspension was stirred again for 1 hour and then transferred to a 100 mL autoclave. The hydrothermal reaction was carried out at 110 °C for 4 h for crystallization and directional etching. The collected white product was washed twice with diluted 1 mmol/L NaOH solution and water. Finally, the product was placed in an oven and calcined at 350 °C at a heating rate of 1 °C/min for 2 h to obtain the white hollow urchin-like TiO_2 .

Nanocage TiN was obtained via the following steps. Hollow urchin-like TiO_2 powder weighing 1 g obtained via the previously described preparation method was placed in a tube furnace. Under the protection of nitrogen, ammonia gas was introduced therein. The temperature was increased to 600 °C at a heating rate of 5 °C/min. Under these conditions, the reaction was allowed to proceed for 3 h and the product was allowed to cool naturally to room temperature. Finally, nanocage TiN was obtained.

The phase analysis of the sample was performed using X-ray diffraction (XRD) on Bruker D8 Discover diffractometer (Germany) with $\text{Cu K}\alpha$ radiation. Scanning electron microscopy (SEM) and energy-dispersive X-ray spectroscopy (EDS) were performed using Hitachi S-4800 instrument (Japan). Transmission electron microscopy (TEM) and selected-area electron diffraction (SAED) were performed using a JEOL F200 electron microscope (Japan)

operating at 200 kV. Ultraviolet-visible (UV-vis) absorption spectra were obtained using a Shimazu UV-3600 Plus spectrophotometer (Japan). A Renishaw in Via Qontor laser confocal micro-Raman spectrometer (USA) was used to determine the SERS properties of the nanocage TiN. In addition, for SERS detection, the laser excitation wavelength was 532 nm, the laser power was 0.7 mW, and the magnification of the objective lens was $\times 100$. In order to improve the signal reproducibility and uniformity of the SERS substrate, the nanocage TiN substrate was added to the probe molecule aqueous solution for measurement and maintained for 20 minutes. In all SERS detections, the laser beam was perpendicular to the top of the sample, and the beam spot diameter was about 5 μm .

3. Results and discussion

The TiO_2 synthesized by the hydrothermal method is a white precipitate, as shown in the inset of Fig. 2a. The X-ray diffraction (XRD) pattern (Fig. 2a) shows that these white precipitates are amorphous TiO_2 nanospheres. SEM images show that the white precipitate is composed of uniformly distributed spheres with a diameter of 200-300 nm (Fig. 2b-c).

After chemical etching, the amorphous TiO_2 nanospheres transformed into a hollow urchin-like structures, and the samples were white, as shown in the inset of Fig. 2d. The XRD pattern (Fig. 2d) shows that the crystal phase of the white sample can be labeled as anatase

TiO₂ containing rutile phase. Hollow puncture ball structure of the TiO₂ were obtained via SEM, as shown in

Fig. 2e–f. The length of the burrs and diameter of the ball are about 60 nm and 400–600 nm, respectively.

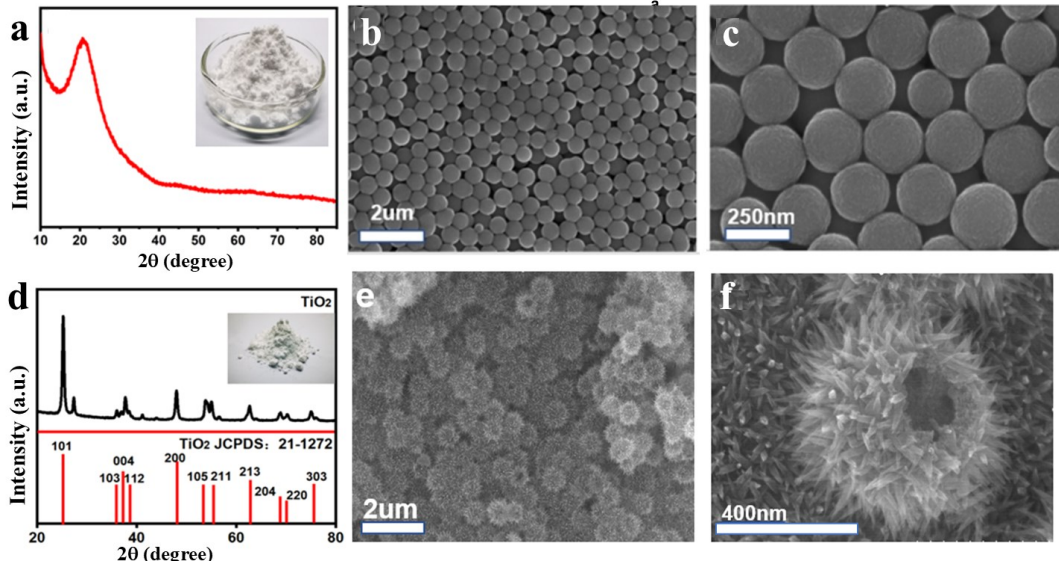


Fig. 2. (a) XRD pattern of amorphous TiO₂ nanospheres, the inset shows the amorphous TiO₂ nanospheres powder; (b-c) SEM image of amorphous TiO₂ nanospheres; (d) XRD pattern of hollow urchin-like TiO₂, the inset shows the hollow urchin-like TiO₂ powder; (e-f) SEM image of hollow urchin-like TiO₂ (colour online)

After nitridation, the urchin-like TiO₂ transformed into nanocage TiN. The obtained black powder as shown in the inset of Fig. 3a. The XRD pattern (Fig. 3a) shows that these products can be clearly indexed as face-centered cubic TiN. The obtained diffraction peaks are well-defined, indicating high crystallinity of the sample. In addition, there are no other diffraction peaks, indicating that the purity was very high, and no other impurities were mixed. The SEM image shows that the surface of the precursor urchin-like TiO₂ was composed of a layer of spines, and the interior was empty as shown in the Fig. 2f. After nitridation, the spines began to melt due to the erosion of high temperature and ammonia, and formed a nanocage

shape composed of particles as shown in the Fig. 3b and 3c. Based on a transmission electron microscopy (TEM) image (Fig. 3d), TiN presents a hollow nanosphere. The surface of the nanospheres was rough and composed of nanoscale particles. The rough surface can enhance the intensity of the local electromagnetic field and generate numerous hotspots. This is beneficial to improve the SERS effect. In addition, as presented in Fig. 3e, the EDS result shows that the atomic ratio of Ti and N was 0.9, which was close to the proportion of TiN. Moreover, X-ray photoelectron spectroscopy (XPS) (Fig. 3f) confirmed the presence of TiN in the black sample.

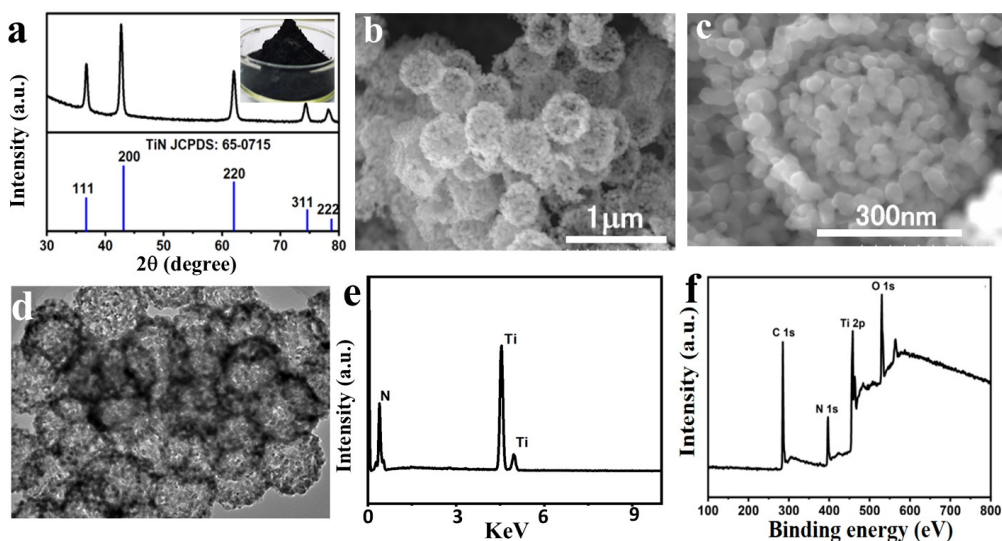


Fig. 3. (a) XRD pattern of nanocage TiN, the inset shows the nanocage TiN powder; (b-c) SEM image of nanocage TiN; (d) TEM image of nanocage TiN; (e) EDS spectrum and (f) XPS of nanocage TiN

Previous research shows that TiN exhibits strong metallicity [10-11]. Additionally, the simulated electron localization functions also shows that the structure of TiN exhibits a high density of free electrons [9]. Owing

to these characteristics and the rough surface, the nanocage TiN exhibited a strong LSPR effect in the visible-light region, with a peak at 512 nm, as shown in Fig. 4a.

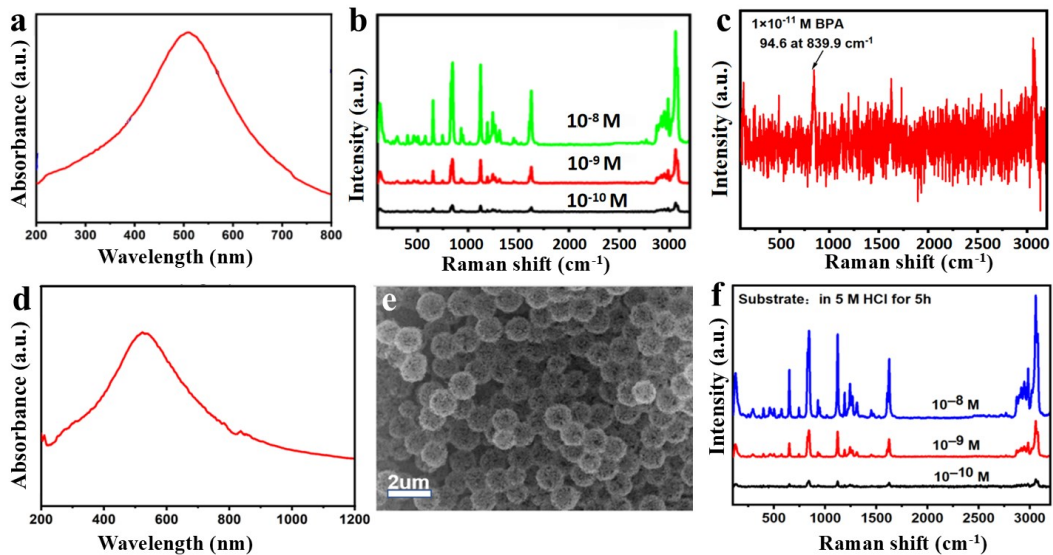


Fig. 4. (a) UV-vis absorption spectrum and (b) substrate reaction to different concentrations of BPA of the nanocage TiN. (c) Resolvable Raman signals of the nanocage TiN as analyte concentration was diluted to 1.0×10^{-12} M. (d) UV-vis absorption spectrum, (e) SEM and (f) Resolvable Raman signals of nanocage TiN after being treated with hydrochloric acid (5 M) (colour online)

The SERS effect of nanocage TiN was investigated. Considering the formation of strong electromagnetic 'hot spots' in the closely arranged nanocage TiN, the Raman scattering signal of the analyte molecules adsorbed at these positions will be greatly enhanced under the stimulation of excitation light. Bisphenol A (BPA), a carcinogenic persistent environmental pollutant, is widely used Raman probe. The SERS performance of a substance can be determined by its sensitivity to BPA. To enhance the resonance Raman effect, a 532 nm laser was selected to closely match the sample's UV-vis absorption peak, with a power of 0.7 mW. The laser beam was placed perpendicular to the top surface of the sample with the magnification of the objective lens being $\times 100$. Different concentrations of BPA samples (10^{-8} – 10^{-11} M) were selected as probe molecules. As shown in Fig. 4b, the nanocage TiN exhibit highly sensitive Raman scattering effects for a series of BPA samples at the concentrations of 10^{-8} , 10^{-9} , and 10^{-10} M. Even at a concentration of 10^{-11} M, nanocage TiN responded well to the analyte ($S/N \geq 4$), as shown in Fig. 4c. It means that the nanocage TiN has excellent SERS performance. It is worth mentioning that the detection limit is better than most semiconductor SERS substrates, and even better than some noble metal substrates.

From the perspective of application, the stability of materials is an important factor. It is worth mentioning that the nanocage TiN microspheres have high chemical stability. The UV-vis absorption spectrum and SEM

images of the nanocage TiN treated with hydrochloric acid (5 M) for 5 h each are shown in Fig. 4d and Fig. 4e. The results show that the nanocage TiN microspheres still exhibited a strong surface plasmon resonance effect and high structural integrity even after severe corrosive procedures, thus demonstrating its excellent acid-treated resistance. The treated nanocage TiN microspheres were used to synthesized SERS substrates, and Raman measurements were performed on BPA solutions with concentrations of 10^{-8} , 10^{-9} and 10^{-10} M. The Raman spectra in Fig. 4f shows that the acid-treated TiN substrates still exhibited significant enhancement effects on BPA and maintained a good detection limit. This indicates that the SERS substrate comprising these nanocage TiN microspheres can function efficiently in acidic environments.

4. Conclusions

Nanocage TiN microsphere substrates were successfully fabricated via a facile hydrothermal method followed by nitridation. The XRD pattern shows that these products can be clearly indexed as face-centered cubic TiN. The morphology, surface plasmon resonance, and SERS were characterized. The results showed that the TiN hollow spheres exhibited excellent SERS performance and a strong LSPR effect in the visible-light region. Furthermore, they were extremely sensitive to typical

environmental pollutant bisphenol A even for a minimum detectable concentration of 10^{-11} M. In addition, the substrate exhibited remarkable corrosion resistance, thus rendering it suitable for application to demanding environments.

Acknowledgment

The work is supported by Zhejiang Provincial Natural Science Foundation of China (Nos. LY21F010010).

References

- [1] X. X. Han, R. S. Rodriguez, C. L. Haynes, Y. Ozaki, B. Zhao, *Nat. Rev. Methods Primers* **1**, 87 (2021).
- [2] Bhavya Sharma, M. Fernanda Cardinal, Samuel L. Kleinman, Nathan G. Greeneltch, Renee R. Frontiera, Martin G. Blaber, George C. Schatz, Richard P. Van Duyne, *MRS Bulletin* **38**, 615 (2013).
- [3] C. Lin, Y. Li, Y. Peng, S. Zhao, M. Xu, L. Zhang, Z. Huang, J. Shi, Y. Yang, *J. Nanobiotechnol.* **21**, 149 (2023).
- [4] H. Guan, W. Li, J. Han, W. Yi, H. Bai, Q. Kong, G. Xi, *Nat. Commun.* **12**, 1376 (2021).
- [5] Q. Kong, D. Liu, L. Yang, H. Zhao, J. Zhang, G. Xi, *J. Phys. Chem. Lett.* **14**(49), 10894 (2023).
- [6] Y. Zhou, S. Yang, *Spectrochim. Acta A* **327**, 125322 (2025).
- [7] H. Guan, W. Yi, T. Li, Y. Li, J. Li, H. Bai, G. Xi, *Nat. Commun.* **11**, 3889 (2020).
- [8] M. Asadizadeh, S. Khosravi, S. Abharian, M. Imani, J. Shakeri, A. Hedayat, N. Babanouri, T. Sherizadeh, *Granul. Matter.* **25**, 21(2023).
- [9] Y. Zhou, S. Wang, Y. Yu, X. Teng, *Appl. Surf. Sci.* **661**, 160071 (2024).
- [10] H. Song, P. Gu, X. Zhu, Q. Yan, D. Yang, *Physica B: Condensed Matter* **545**, 197 (2018).
- [11] A. Valour, M. A. U. Higuita, G. Guillonneau, N. Crespo-Monteiro, D. Jamon, M. Hochedel, J. Michalon, S. Reynaud, F. Vocanson, C. Jiménez, M. Langlet, C. Donnet, Y. Jourlin, *Surf. Coat. Tech.* **413**, 127089 (2021).

*Corresponding author: zhouyun@cjlu.edu.cn
zhouyun@zime.edu.cn